



Computational studies aimed at defining bridging requirements for steel joists

J.R. Eberle¹, R.D. Ziemian², D.R. Potts³

Abstract

The Steel Joist Institute (SJI) specification's bridging criteria for open web steel joists are based on conservative analyses completed several decades ago. These criteria have been recently updated in the 43rd edition of the SJI catalog. In an effort to investigate the accuracy and reliability of such design provisions, the Research Committee of the SJI has funded the authors with a multi-phase project that is aimed at determining the feasibility of using sophisticated second-order finite element analysis methods to model the stability of steel joists. An initial pilot study determined that computer models with appropriate boundary conditions could be prepared that accurately predict the stability behavior of steel joists that were previously experimentally tested. With a focus on predicting ideal brace stiffness and bracing forces, computational models of systems of one to ten parallel joists with intermittent out-of-plane bracing were then investigated. Studies that evaluate several possible modes of initial imperfections, load type (including gravity and uplift conditions), bridging type (including horizontal and X-bracing), and bridging support conditions were completed. This paper will provide an overview of this research project and provide several conclusions for defining erection-bridging requirements in SJI's Standard Specifications.

1. Modeling Validation

Over the past two years, the Research Committee of the Steel Joist Institute (SJI) has sponsored a research project aimed at exploring the feasibility of using structural analysis software to investigate the behavior of bridging within steel joist systems.

The study began by comparing analysis results with experimental data obtained from prior tests of unbraced open web steel joists (Ziemian, et al 2004). After a thorough study of several joist configurations, it was found that acceptable computational results, including vertical and out-of-plane horizontal deflections, could be obtained using the following analysis parameters:

- All individual chord and web members modeled with 12 degree-of-freedom frame elements.
- Initial imperfection of the compression chord included.

¹ Graduate Research Assistant, Virginia Tech, <jre014@vt.edu>

² Professor, Bucknell University, <ziemian@bucknell.edu>

³ Instructor, Pennsylvania College of Technology, <dpotts@pct.edu>

- Spring elements to model the rotational and flexural stiffness of the connections at the joist end supports.
- Rigorous second-order elastic analysis is employed.

2. Gravity Loading Studies

Having shown the feasibility of using computational analysis to model individual un-braced steel joists, the study then went on to focus on systems of braced joists (Fig. 1).

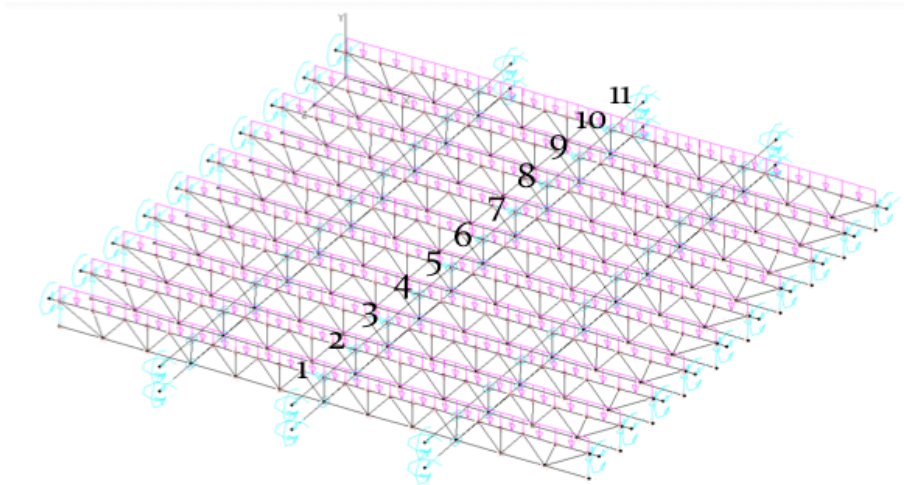


Figure 1: Example of a system of 10 parallel 28K10 joists; out-of-plane bracing numbered in black

Two rather slender joist configurations were selected for investigation, an 18K3 with a span of 28'-3" and a 28K10 with a span of 48'-0". These joists provide a range of span lengths and also provide a variation in joist geometry, with the 18K3's comprised of round-bar webs and the 28K10's including crimped-angle web members. Applying the provisions of the SJI Standard Specification, the required number of horizontal bridging rows required during construction loading for systems of 18K3's and 28K10's were determined to be two and three, respectively (*Standard Specifications* 2005). To get forces to develop and accumulate in the rows of bridging, it was necessary to impose an initial out of straightness of $L_b/480$ in the compression chord⁴ (Fig. 2).

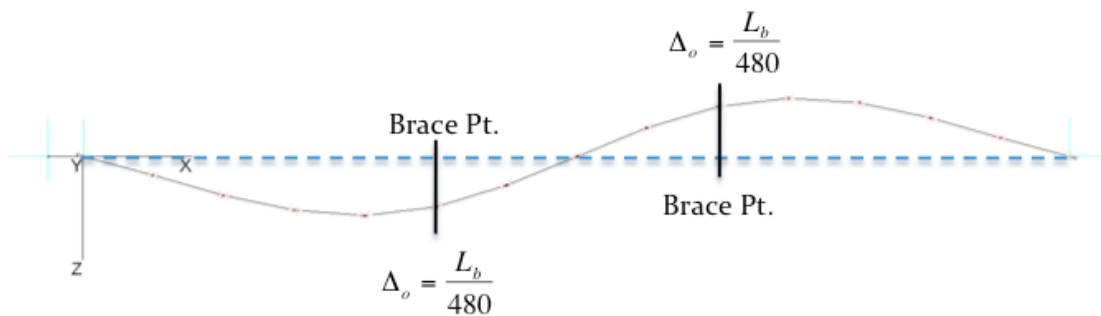


Figure 2: Plan view of an 18K3 defining initial out of straightness imposed on top chord

⁴ Unbraced length L_b is defined as the distance between points of bridging.

Applying a uniformly distributed gravity load along the top chord of the joists, these models were then used to compute the ideal brace stiffness⁵ for the bridging members. Starting with a minimal bracing stiffness that results in single-wave buckling of the compression chord, this process is completed by performing rigorous second-order elastic analyses for incremental amounts of bracing stiffness until this controlling mode changes to multi-wave buckling of the compression chord about the brace points. In all cases, bracing stiffness is defined by the axial stiffness of the bridging members given by:

$$\beta = \frac{EA}{L} \quad (1)$$

where E is the modulus of elasticity of the bridging, A the cross sectional area of the bridging, and L the bridging length (spacing of joists).

2.1 Horizontal Bridging

Reasonable values for bracing stiffness were obtained and compared for two conditions, including (i) having only the tension bracing engaged (one end of bridging anchored), and (ii) having both tension and compression bracing engaged (both ends of bridging anchored). It should be noted that several initial imperfection modes of the compression chord were investigated, with the controlling mode defined by all joists in the same reverse curvature shape (Fig. 2). Typical results of the required bridging stiffness and forces are shown in Table 1.

Table 1: Comparison of effects resulting from the inclusion of compression bridging being engaged

	Tension Bracing				Tension and Compression Bracing				Average
	18K3		28K10		18K3		28K10		
	Mode 1	Mode 2	Mode 1	Mode 2	Mode 1	Mode 2	Mode 1	Mode 2	
β_i^{system}	20.54	21.15	72.50	72.50	5.26	5.98	19.82	19.82	
$F_{\text{brace}}^{\text{max}}$	0.83	2.88	0.12	4.46	0.43	1.46	0.05	2.28	
	% of original β_i^{system}				25.6%	28.3%	27.3%	27.3%	27.1%
	% of original $F_{\text{brace}}^{\text{max}}$				52.5%	50.7%	46.5%	51.1%	50.2%

1. Modes 1 and 2 represent compression chord initial imperfection shapes of single sweep and reverse curvature (Fig. 2), respectively
2. β_i^{system} represents the ideal bracing stiffness (k/in) for the system of parallel joists (in this case 10 joists were investigated)
3. $F_{\text{brace}}^{\text{max}}$ represents the largest absolute magnitude of bracing force observed within the system (kips)
4. The percent of original values represent the reduction in required bracing stiffness and resulting force observed by including compression anchorage for the bracing.

Although bracing forces were calculated for two levels of bridging stiffness (1.1 and 2.0 times the ideal brace stiffness), it is suggested that bracing forces come from the latter brace stiffness ($2\beta_i$). Table 1 shows that engaging both the tension and compression bracing significantly reduces the required bridging stiffness. For a 10-joist system, the required stiffness is nearly cut to a quarter of the stiffness required for a system with only tension bracing engaged and the bracing forces are reduced by approximately half.

⁵ Ideal brace stiffness β_i is defined as the stiffness of the bridging at which the controlling buckling mode transitions from compression chord buckling in a single sway mode to compression chord buckling about the location of the brace points.

With an increased confidence in the computational models, the SJI Research Committee requested that two parameters be studied, including (i) the impact of the initial imperfection magnitude, and (ii) the magnitude of the applied gravity load (which for a linear elastic analysis is directly proportional to the top chord axial stress). With the respect to the latter, the increasing nonlinear relationships shown in Fig. 3 were obtained. Similar results were obtained when the magnitude of the initial imperfection was varied.

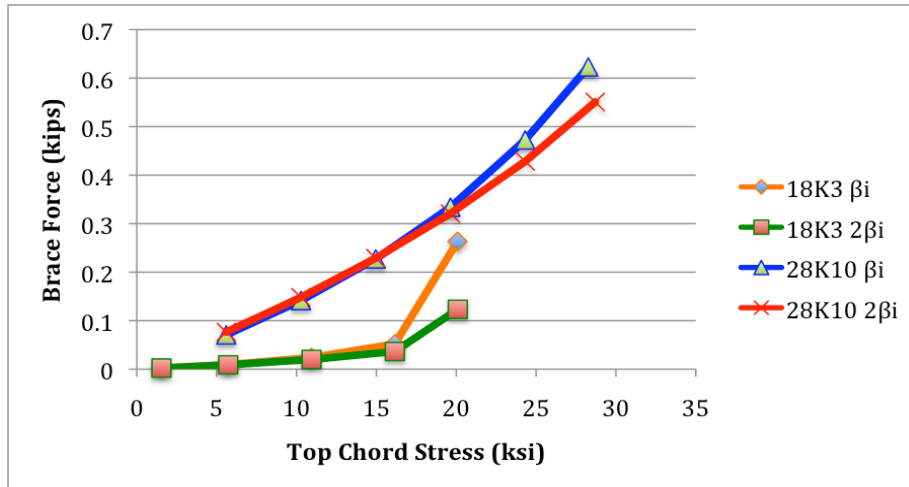


Figure 3: Plot depicting nonlinear relationships for the magnitude of applied gravity load study

This study also showed the advantage of using twice the ideal brace stiffness, especially with gravity loads that result in large compression chord axial stresses. In general, increasing the bracing stiffness results in a decrease in brace forces. Although this observation may be contrary to intuition, it is the result of reducing second-order effects; as the stiffness of the bridging is increased, the amount that the joist can lean is reduced and therefore second-order overturning effects are reduced.

With the above studies completed, the SJI Research Committee further requested that the computational models be used to review a common assumption that bridging forces do not accumulate over more than 8 joists. Using a system of 10 joists, computational studies that included both tension only bracing and tension/compression bracing show that bridging forces do indeed continue to accumulate over a system of joists in a fairly linear fashion (Fig. 4), with little to no indication of accumulating forces diminishing. It is important to note that the computational models assumed all initial imperfections in the same direction and magnitude, which in real-field conditions is most likely, not the case.

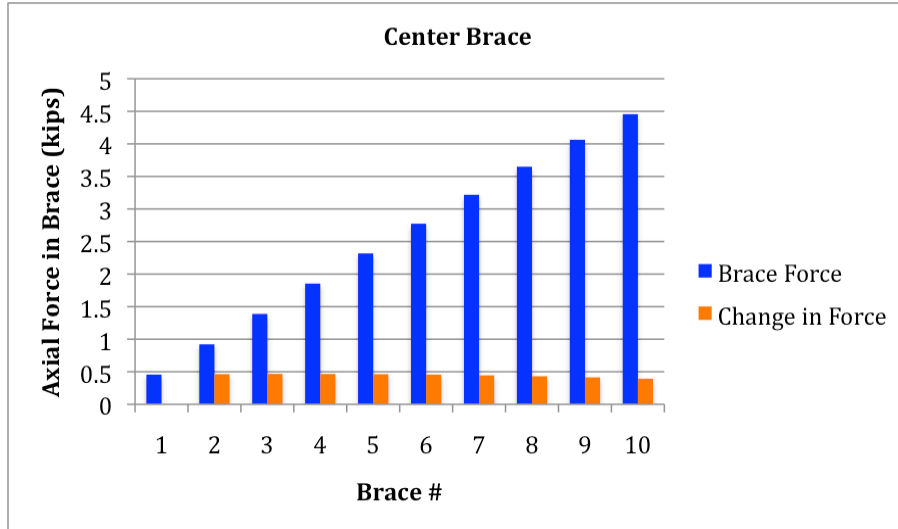


Figure 4: Accumulation of bracing forces for a system of 10 parallel 28K10's with only the tension bracing engaged and the bracing stiffness equal to twice the ideal bracing stiffness; brace numbers are defined in Fig. 1

The SJI Research Committee also requested that the impact of the stiffness of the brace anchorage conditions be studied through the use of these computational models. By considering several different levels of anchorage stiffness, it was shown that the brace anchorage could have a significant effect on the behavior of the joist systems. It was also shown that the computational analysis could be used to define stiffness requirements for anchorage systems, with several simple design examples prepared.

2.2 X-Bridging

With the horizontal-bridging gravity-load studies complete, the SJI Research Committee requested that pilot studies using continuous X-bridging within parallel joist systems (Fig. 5) be completed.

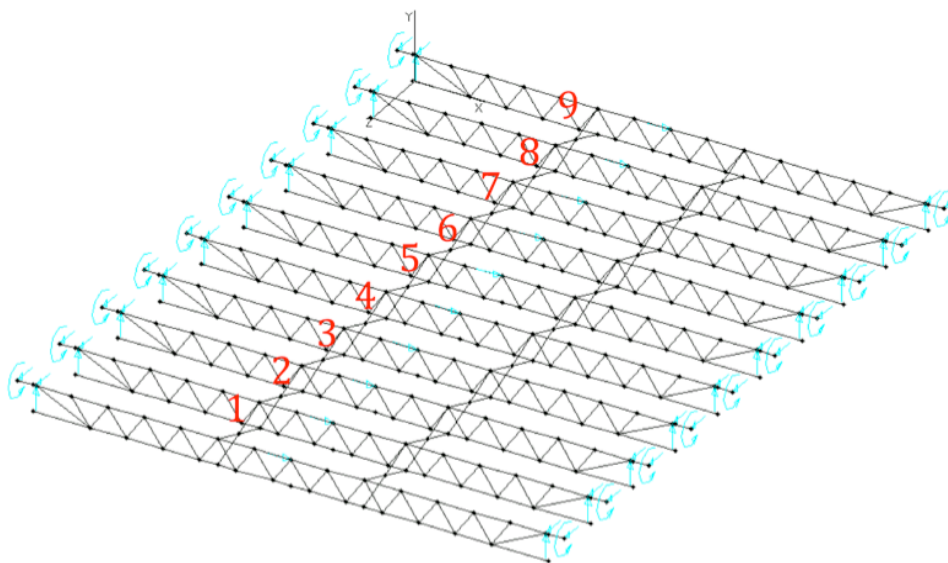


Figure 5: X-bridging with no anchorage implemented on system of 10 parallel joists; X-bracing numbered in red

The geometry of structural X-bridging allows joist systems to be self-stabilizing and allows for 3 conditions of bridging anchorage to be studied, including (i) no anchorage, (ii) tension-side anchorage (joist imperfections leaning away from anchorage), and (iii) both sides of bridging anchored. Because tension and compression are induced within the components of the X-bridging, it was necessary to provide a value for the bending stiffness of the compression bracing in order to avoid brace buckling. To determine the appropriate bending stiffness, a standard bracing angle size was chosen by limiting the L/r ratio to 200 as defined in the SJI Specification (*Standard Specifications* 2005). After defining the appropriate bending stiffness for each of the braces within the model, the ideal bracing stiffness corresponding to system instability could be determined for each of the given cases. As in previous studies, analyses were conducted using an axial bracing stiffness of $2\beta_i$ for the given system. For all X-bridging studies, analyses were conducted using a uniformly distributed gravity load that caused buckling of the compression chord about the brace points and all reported brace forces were taken at this full critical load.

The unique nature of X-bridging allows the bracing forces to be resolved through minor axis bending of the upper and lower chords of the joists. As a result, no end-anchorage is required (first case investigated). It should be noted that this would be typical for a joist system centrally located in a wide building that includes expansion joints. The no-anchorage case required the largest ideal bracing stiffness's of 0.94 k/in and 3.48 k/in for the 18K3 and 28K10 joist systems, respectively. The distribution of bracing forces across the system showed that these forces did not accumulate (Fig. 6).

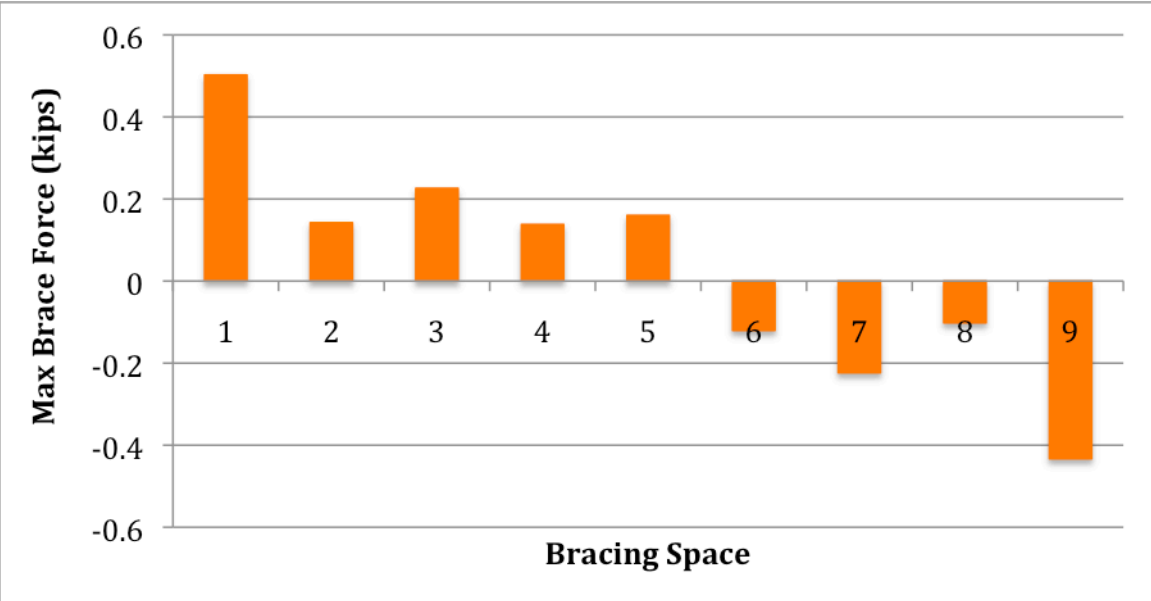


Figure 6: Maximum bracing force observed within X-bridging as a function of bracing space for the 18K3 system of joists and no anchorage present; brace numbers defined in Fig. 5

The largest brace forces were observed in the spaces near the end joists due to the fact that the end joists had X-bridging on only one side; the magnitude of all other brace forces were approximately equal. It was also observed that the maximum bracing forces switched from compression to tension in the middle of the system.

The second case of X-bridging investigated included anchoring the system with horizontal bridging attached on one side such that the joist imperfections leaned away from the anchorage. This case of bridging fixity would correspond to an end system of joists located outside of an expansion joint. The required bracing stiffness for this case was slightly less than the previous case with values of 0.85 k/in and 1.79 k/in for the 18K3 and 28K10 joist systems, respectively. Within this system of joists the largest bracing forces were found to be nearest the end that was not anchored, as would be expected from the previous findings in the studies of the un-anchored systems. Following the largest brace force, the remaining bracing forces held fairly linear to the anchorage.

Anchoring both ends of the X-bridging with horizontal bridging was the final case investigated. This anchorage case would be typical of smaller joist systems where no expansion joints are necessary and there is a reliable anchorage point on both ends of the system. Because both sides are anchored, the large bracing forces (and corresponding displacements) were not present as in the previous cases in which there was an un-anchored end (Fig. 7). Due to this fact, a significant reduction in ideal bracing stiffness was observed with values found to be 0.30 k/in and 0.56 k/in for the 18K3 and 28K10 joist systems, respectively.

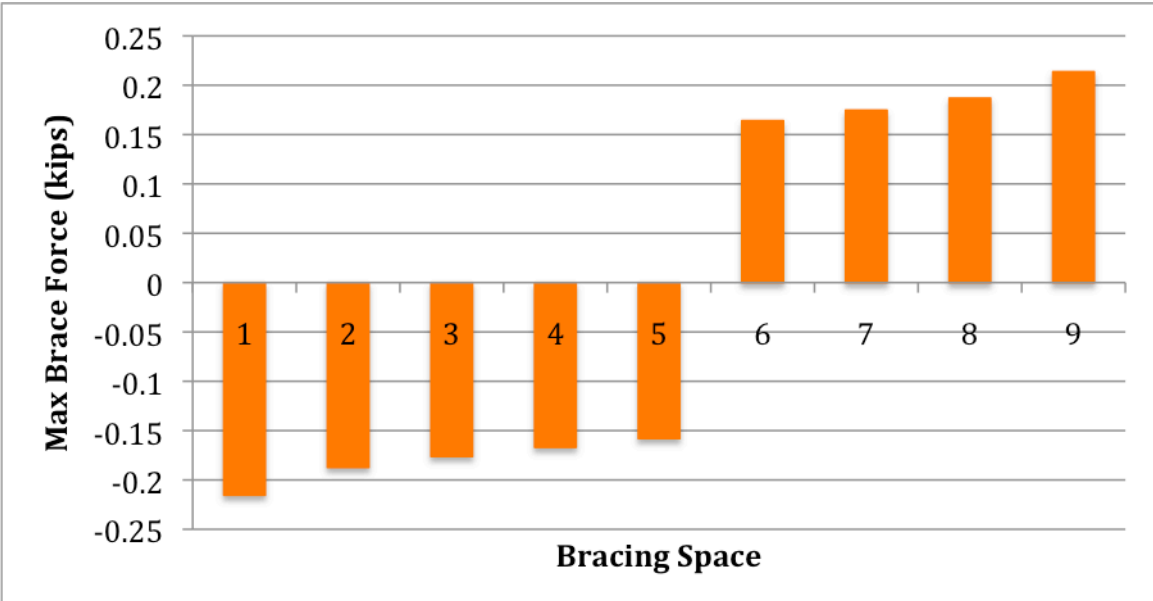


Figure 7: Bracing forces as a function of bracing space for the 18K3 system of joists with both sides anchored

The distribution of bracing forces again switches from compression to tension at the center bracing location; in this case because both ends of the bridging were fixed allowing both tension and compression anchorage forces to develop. A very slight accumulation of forces was observed within this system with the largest forces near the anchorages. This accumulation, however, is very minor in comparison to the studies conducted for the cases of horizontal bridging. Anchoring both ends of the bridging also greatly reduces the maximum bracing forces within the system.

Finally, a small study was also conducted on a system of joists assuming that only tension bracing was engaged within the X-bridging system. To allow this study to be conducted, the

structural analysis software was modified such that if a brace was placed into compression, the axial stiffness of that member was set to zero thereby resisting no force. Analyses were conducted in a manner similar to the previous X-bridging conditions and only a system with both ends anchored was studied. After conducting several analyses, it was found that bracing forces again accumulated only slightly throughout the system with the largest bracing forces near the supports. As shown in Fig. 8, it was observed that the bracing forces were significantly increased from the system that had both compression and tension bracing engaged (shown previously in Fig. 6).

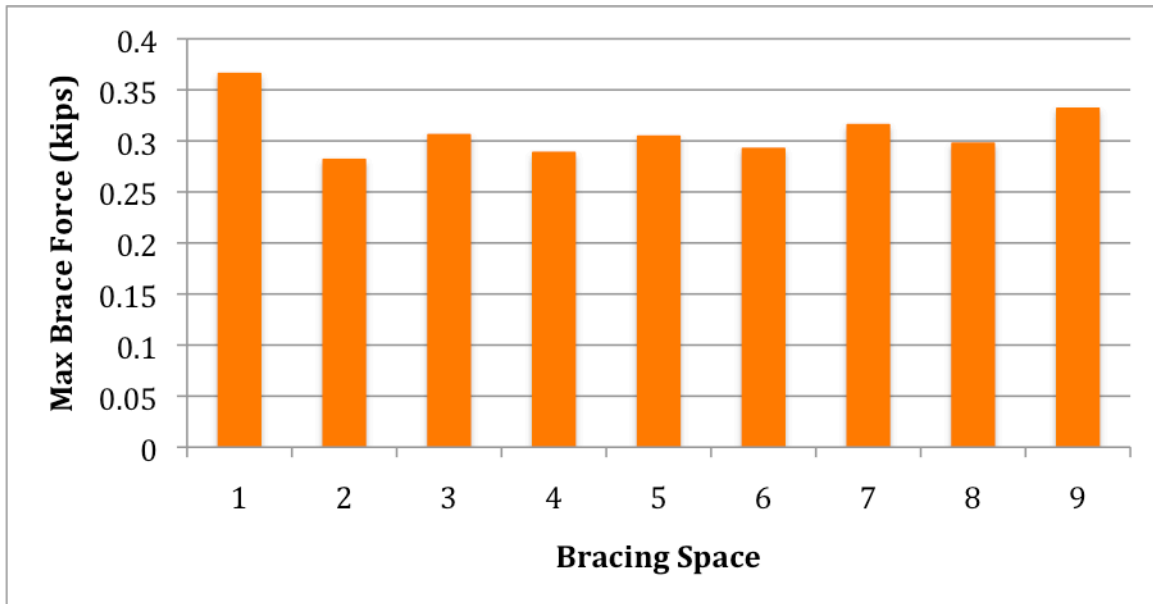


Figure 8: Bracing forces as a function of bracing space for the 18K3 system of joists with only tension bracing engaged

3. Uplift Loading Studies

With the gravity load studies complete, the focus shifted to analyzing the behavior of joist systems subject to net-uplift forces from sources such as wind loads. Similar to the gravity load investigations, uplift loading studies began by considering the behavior of a single joist and progressed to studying systems of 10 parallel joists.

As defined in the SJI Standard Specification, bracing is required at the first lower chord panel points in addition to the lower chord bracing locations already imposed on the joist for gravity loading conditions (*Standard Specifications* 2005). Because of the significant axial and shear stiffness of the deck, the upper chord was modeled as fully laterally braced, which is represented in the finite element model by restraining the out-of-plane displacement at the upper chord panel points. Similar to gravity loading conditions, the analyses include a uniformly distributed load with a magnitude that causes buckling of the compression chord (which for uplift loading would be the lower chord) about bracing locations.

Preliminary uplift analyses indicated an expected failure mode within the joist in which the first-web member (a tension member under gravity loading) of the joist was experiencing buckling

due to the large compression forces induced by uplift loading. Increasing the elastic modulus of the end web members by a factor of 5 to prevent buckling circumvented this failure mode, which in properly designed joists would not occur. With this implementation, the controlling failure mode was always buckling of the bottom chord.

Definition of an initial imperfection in the lower chord is now necessary to allow bracing forces to develop and accumulate as result of uplift loads. Based on input from the SJI Research Committee, an imperfection magnitude of $L_b/480$ was used at the interior bracing locations and $L_e/480$ at the first end-panel bracing locations⁶. With imperfections applied at both the joist ends and along the joist span, four initial-imperfection modes were investigated that included single-sweep and reverse-curvature forms. To choose the worst-case initial imperfection, analyses were conducted on a braced single joist for both the 18K3 and 28K10 configurations. Because the brace forces become unbounded at the failure loads of the joist systems, brace forces were compared at 90% of the applied load, which represents a load in which the joists are nearly unstable but the bracing forces are still well defined. Using this approach, it was found that initial imperfection cases involving a reverse-curvature shape resulted consistently in larger brace forces than cases of a single-sweep imperfection shapes. It was further determined that reverse curvature imperfections with end panel displacements in the opposite direction of the next bracing location (Fig. 9) resulted in a worst-case scenario. It is important to note that these results are consistent with (i) the results found in the gravity-loading studies, and (ii) results found in the literature on beam bracing studies (Wang and Helwig 2005).

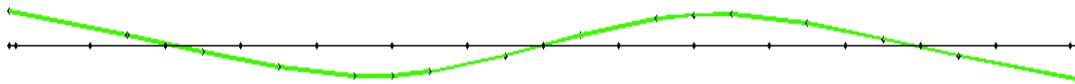


Figure 9: Plan view of controlling initial imperfection shape for uplift loading (18K3)

With an initial imperfection defined for uplift analyses, the project progressed to study systems of ten joists in parallel. At the request of the SJI Research Committee a pilot study was conducted to determine the effects of upper chord rotational restraint provided by structural deck. In this study, the corrugated deck was modeled as a continuous member attached to each joist at the upper chord panel points. The deck's flexural stiffness was varied as a multiple of a calculated deck moment of inertia that was defined by the SJI Research Committee. This multiple was varied from 0 to 5 to encompass a wide range of possible deck stiffness contributions and/or the potential for local material distortion at locations where the deck is connected to the upper chord.

This deck stiffness investigation began by determining the impact of top chord rotational restraint on the elastic critical load capacity of the joist system. As expected the structural system was capable of resisting additional load with increased deck stiffness. The inclusion of deck with a flexural stiffness 5 times that defined by SJI increased the system capacity by as much as 34% and 20% for the 18K3 and 28K10, respectively.

⁶ End panel unbraced length L_e is defined as the distance between the joist end and the first end chord bracing location.

Significant increases in uplift capacity were also observed for minimal increases in deck flexural stiffness (Fig. 10). For example, if half of the SJI flexural stiffness of the deck can be transferred to the joist, an increase in elastic-load capacity of 30% and 15% could be expected for the 18K3 and 28K10, respectively.

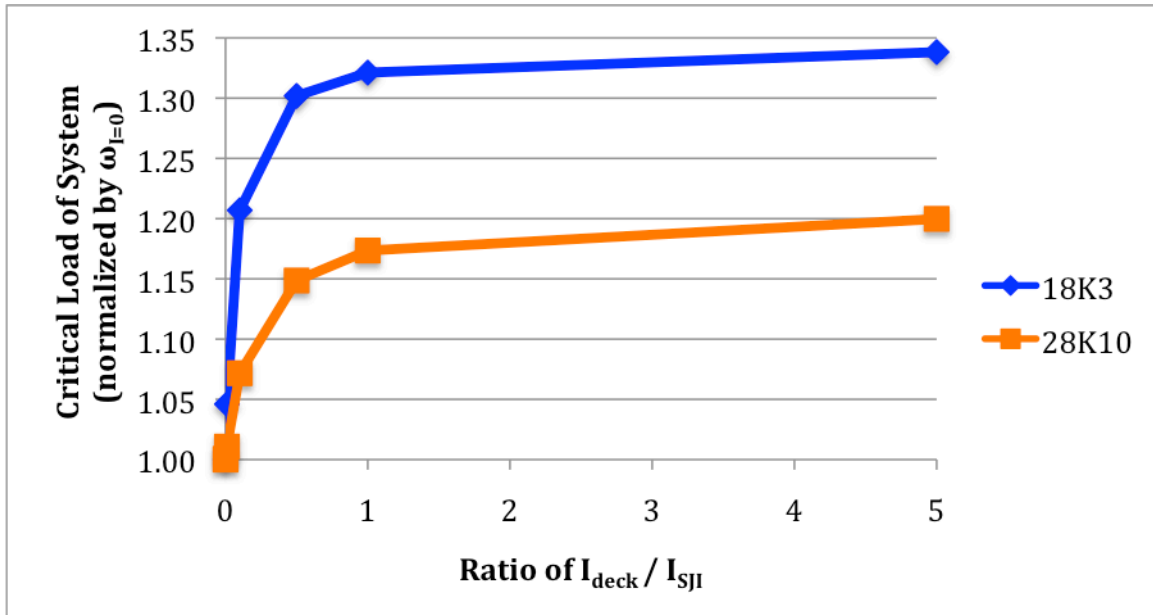


Figure 10: Plot showing effects of deck flexural stiffness on the critical load of the system

The relationship between deck flexural stiffness and ideal bracing stiffness was also investigated. The required ideal bracing stiffness of the system decreased considerably with only small amounts of rotational restraint being provided to the top chord by the presence of structural deck. However, this rather steep reduction in ideal bracing stiffness was soon offset by the need to increase ideal bracing stiffness as a result of the system being able to resist significantly more load. In general, the presence of the deck can decrease the required ideal bracing stiffness by 85% to 95% for the 18K3 and 28K10 joists studied.

The impact of the deck flexural stiffness on required brace force was also studied. In general, the largest bracing forces are observed when there is no deck attached to the joist system. As the flexural stiffness of the deck is increased, the brace forces do decrease and asymptotically approach a single value; indicating a point of diminishing returns. Unfortunately, reductions in brace force of only 2% to 10% were observed for the deck stiffened 18K3 and 28K10 joist systems (Fig. 11).

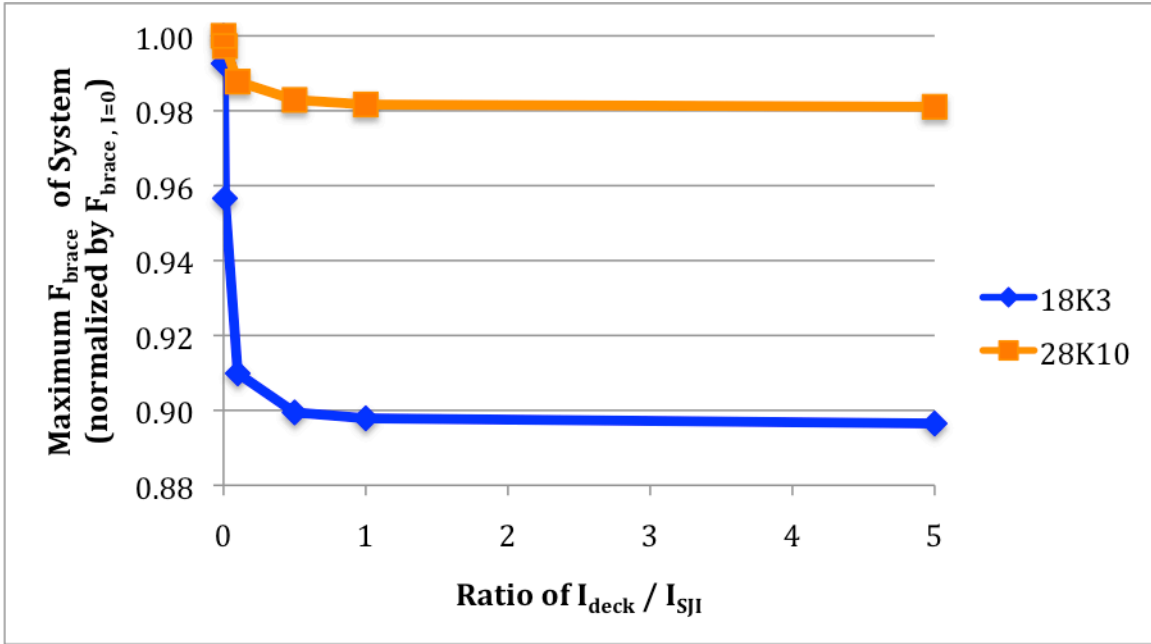


Figure 11: Plot showing the decrease in bracing forces resulting from the addition of deck flexural stiffness

Finally, the accumulation of brace forces due to uplift loading was also studied in relation to deck stiffness with two cases investigated, including no deck and deck stiffness properties defined by SJI. For these two cases, uplift loading analyses were conducted on systems having tension-only bracing engaged and on systems with tension and compression bracing engaged. With these four combinations studied for each joist type, it was observed consistently that bracing forces do accumulate linearly for systems having no deck flexural stiffness and slightly nonlinearly for systems with reasonable deck stiffness. By engaging both tension and compression bracing, the bracing forces decrease by approximately 50% and their distribution remains linear (Fig. 12), which is similar to the results observed for tension-only bracing engaged.

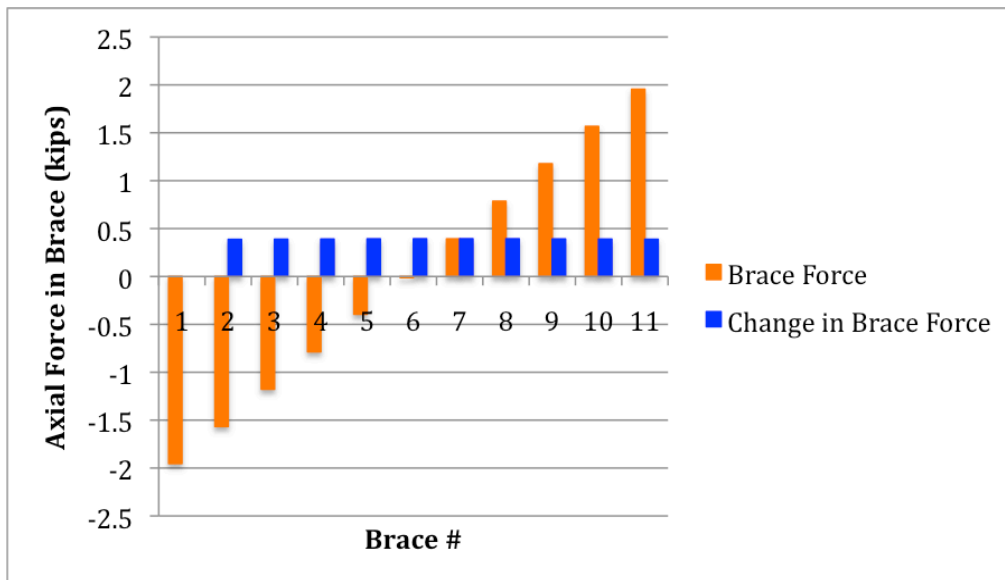


Figure 12: Accumulation of bracing forces for a system of 10 parallel 28K10 joists with deck stiffness included

With these preliminary uplift studies complete, the SJI Research Committee requested a series of uplift studies that focus on the potential reduction in bracing forces resulting from (i) a reduction in applied load, (ii) a reduction in initial imperfection, and (iii) imperfections applied to only a limited number of the joists within a system.

3.1 Reduced Applied Load

As defined by the SJI Research Committee, a reduction factor of 0.9 was imposed on the uniformly distributed uplift loading applied to the structural system. In effect, this load represents 90% of the load that would cause buckling of the lower (compression) chords of the joists about the bracing points. For analyses of this system, a bracing stiffness of twice the ideal braced stiffness $2\beta_i$, as determined from the previous studies conducted on systems without a reduced load, was implemented. After conducting second-order elastic analyses on the joist systems, the maximum bracing force was taken at 90% of the applied load to once again avoid the wide variation of forces near the critical load and to also allow for comparison to the bracing forces found for joist systems previously studied that did not include a reduction in load. From these results, it was determined that the relationship between applied load and bracing force is approximately linear. By reducing the applied load to 90% of the original load, the maximum brace forces were reduced to 88.3% and 88.9% of the original brace force for the 18K3 and 28K10 parallel joist systems, respectively.

3.2 Reducing Magnitude of Initial Imperfections

It seems reasonable that the magnitude of the initial imperfection imposed on a system of joists can be reduced to account for the unlikeliness that all joists will lean in the same direction and with a maximum initial imperfection. For the parallel systems studied, the SJI Research Committee decided on an initial imperfection of $0.453\Delta_o$, where $\Delta_o (=L_b/480)$ is the maximum initial imperfection used in the above studies. This reduced initial imperfection was imposed in the same direction on all 10 joists within the system and analyses were conducted using uplift loading conditions. The ideal bracing stiffness found for systems with this reduced initial imperfection was only slightly different (approximately 4%) than for systems with the full initial imperfection ($\Delta_o=L_b/480$). For comparative purposes, the brace forces were taken at 90% of the applied critical load, which was again done to avoid the wide variation of forces at the critical load. It was determined that initial imperfection magnitude and bracing force are very close to being linearly related. By reducing the initial imperfection magnitude to 45.3% of Δ_o , the bracing forces were reduced to 44.9% and 44.8% of the original bracing forces for the 18K3 and 28K10 systems, respectively.

3.3 Reducing Number of Imperfect Joists Within a System

As an alternative method for accounting for the fact that it is unlikely that all joists will lean in the same direction with a maximum magnitude, the Canadian Institute of Steel Construction specification (*Handbook of 2011*) permits imposing an imperfection on some but not necessarily all joists within a system. This method involves imposing the full initial imperfection of $\Delta_o=L_b/480$ on \sqrt{n} joists within the system, where n represents the total number of parallel joists within the system. For the 10 joist systems investigated under uplift loading conditions, the number of imperfect joists could be taken as 4.

To determine which 4 of the 10 joists should include the imperfections, a simple leaning column study was conducted with a single row of horizontal bracing. This column example showed that placing the imperfect columns farthest from the lateral support system produced the largest bracing forces. Translating this principle to the joist study, however, proved problematic due to the multiple brace points being anchored on alternating sides of the system (Fig. 13). With such anchorages on both sides of the system, there were two possible orientations of imperfect joist configurations to study including (i) 4 imperfect joists all located next to each other near one of the anchorages, and (ii) simply alternating between straight and imperfect joists. A study of these two orientations showed that the ordering of imperfect joists was not a significant factor for the specific joist configurations being investigated.

With this information, analyses for comparing bracing forces were conducted with a bracing stiffness of $2\beta_i$ and bracing forces were again taken at 90% of the critical applied load. It was determined that the number of imperfect joists within a system and the amount of bracing force are very closely correlated. By reducing the number of imperfect joists from 10 to 4 within a 10-joist system, the bracing forces were reduced by approximately 60%.

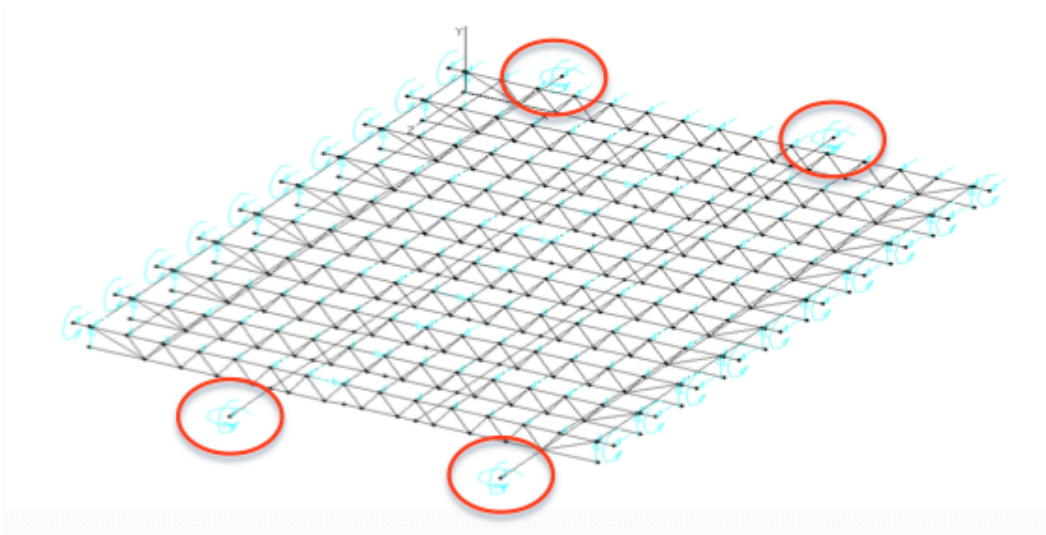


Figure 13: Parallel system of joists showing anchorage on opposing sides

4. Short Span Joist Studies

In the most recent phase of this research, studies were conducted to investigate the bridging requirements for short span steel joists, which are generally defined by the SJI as joists with a span less than or equal to 30 ft. Specifically, the load carrying capacities of these joists subject to various bridging conditions were to be determined. All cases investigated for this study were conducted on single joists with top and bottom chord bridging (as applicable) modeled as out-of-plane pinned supports. Joists were subjected to uniformly distributed gravity loads applied to the top chord. The initial imperfection required to develop bracing forces was defined by the SJI Research Committee as the sum of the top chord imperfection resulting from buckling analysis and a 0.25" to 12" pitch to account for possible sloped roof conditions (Fig. 14).

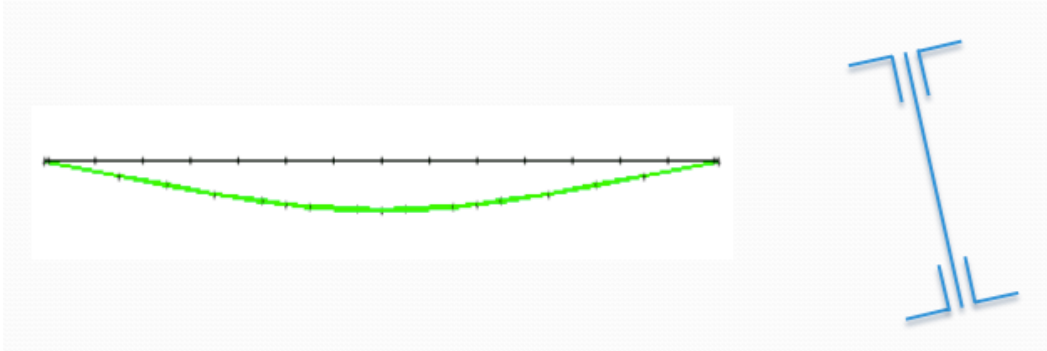


Figure 14: Components of initial imperfection including buckling analysis result (left) and joist pitch (right)

For this study, the 18K3 with a span of 28'-3" (used in the previous research) was investigated along with a 10K1, 12K1, and 14K3 with spans of 19'-10", 22'-0", and 28'-0", respectively. Because of their short spans, all of the joists investigated are fabricated with round bar web members. Deck scenarios of (i) no deck diaphragm and (ii) deck diaphragm present (modeled as top chord fully restrained out-of-plane) were investigated. For both deck scenarios, a case with no bridging provided was used to investigate the necessity of bridging for both erection stability as well as design load stability. In the case of the deck diaphragm being present, additional bridging considerations of one row of lower chord bridging at mid-span and two rows of bridging at the lower chord end panel points were considered. For the case of two rows of bridging, these rows were placed at the lower chord end panel points due to the necessity of bracing those panels for uplift loading.

Second-order inelastic analyses were conducted with reduction factors of 0.9 and 0.8 applied to the materials yield strength and modulus of elasticity, respectively. From the analyses conducted, the failure load and mode for each case was obtained. To account for the possibility of individual members buckling, each member was subdivided into 8 elements (Fig. 15).

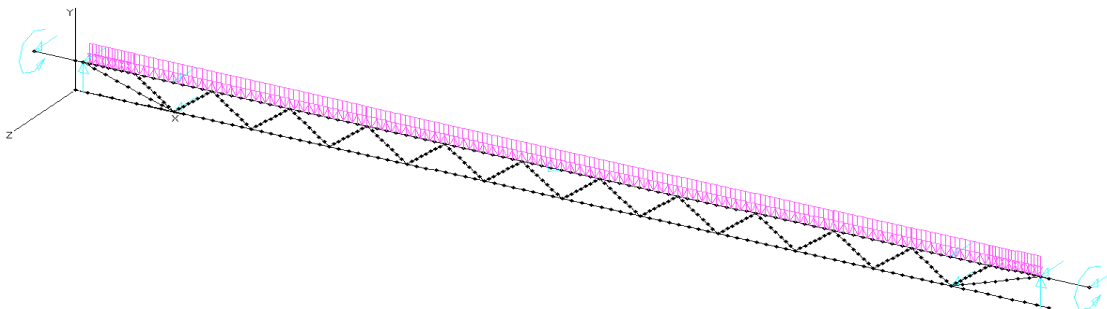


Figure 15: Single joist model used in short span joist study

After all cases were investigated, three failure modes were generally observed, including (i) top chord buckling, (ii) bottom chord yielding, or (iii) web sideways buckling. Results for the short span joist studies are shown in Tables 2 and 3.

Table 2: Results for short span joist study with no deck diaphragm present (erection stability)

	No Bridging	
	Failure Load	Failure Mode
10K1	180	TCB
12K1	56.4	TCB
14K3	81.6	TCB
18K3	52.8	TCB

1. Failure loads given in lb/ft
2. TCB represents top chord buckling failure mode

Table 3: Results for short span joist study with deck diaphragm present (design loads)

	1 Row Bridging		2 Rows Bridging		No Bridging		SJI LFRD Design Load
	Failure Load	Failure Mode	Failure Load	Failure Mode	Failure Load	Failure Mode	
10K1	302	BCY	302	BCY	269	BCY	298 (2)
12K1	340	TCB	336	TCB	202	WSB	298 (2)
14K3	264	BCY	264	BCY	196	WSB	270 (3)
18K3	341	BCY	341	BCY	238	WSB	351 (3)

1. Failure loads and SJI LFRD design loads given in lb/ft
2. TCB represents top chord buckling failure mode
3. BCY represents bottom chord yielding failure mode
4. WSB represents web sidesway buckling failure mode
5. The number in parenthesis next to the SJI LFRD design load represents the number of required bridging rows defined by the SJI specification

As expected, top-chord buckling controls for the cases where the deck diaphragm is not present. When the deck diaphragm is present, however, web sidesway buckling is the controlling failure mode for all cases where no bottom chord bridging is provided. This phenomenon is the result of the tension forces in the bottom chord being offset vertically by the initial imperfection from the top chord. With the top chord restrained and unable to buckle globally, the bottom chord displaces out-of-plane and failure ensues. When bridging is applied to the bottom chords, web sidesway buckling is prevented and bottom-chord yielding controls. This change occurs regardless of the number of bridging rows applied; indicating that it only takes a small amount of bottom-chord restraint to prevent web sidesway buckling from occurring. In being able to achieve bottom-chord yielding, the failure load is significantly increased to values comparable to the design loads given by SJI. The failure load of the joist also appears to be independent of the number of rows of bridging (when bottom chord yielding controls), further supporting the fact that even one row of bottom-chord bridging may provide adequate out-of-plane stability for the system.

It is interesting to note that the 12K1 never achieved bottom-chord yielding. Unlike the other joists studied, it has equal size top and bottom chords. Given that the resulting magnitudes of the top- and bottom-chord axial forces are also approximately equal, inelastic buckling will always control over cross-section yielding, regardless of the presence of bridging and/or deck diaphragm.

The research on short-span joists concluded with investigations of two additional items related to web sidesway buckling, including studying the effects of (i) the flexural stiffness of the deck on failure load/mode, and (ii) the bottom chord radius of gyration on web sidesway buckling.

4.1 Impact of Deck Flexural Stiffness

As in previous studies, the deck flexural stiffness was varied as a multiple of the value provided by the SJI Research Committee. Given that this specific study would only investigate single joists, it was necessary to model deck flexural stiffness with equivalent rotational springs (Fig. 16). These springs were provided at panel and/or mid-panel points to allow for the 36 in. minimum spacing of deck attachment points as required by the SJI Specification (*Standard Specifications* 2005).

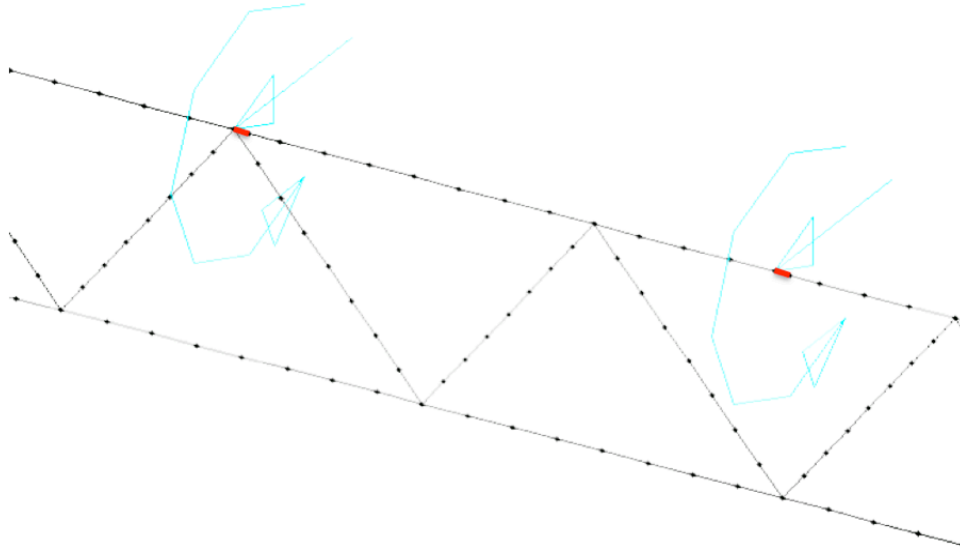


Figure 16: Deck flexural stiffness modeled by rotational springs shown in red (solid)

A summary of the results from this study is provided in Table 4. By including only a small percentage (1%) of the anticipated deck flexural stiffness the joists can nearly reach their design loads and failure modes of bottom chord yielding. The small 2.3% to 3.6% differences between analysis failure loads and the SJI design loads can be attributed to many factors, including the yield surface employed in MASTAN2 and small amounts of bending in the bottom-chord contributing to the formation of plastic hinges. In general, these findings further support the above observations that only a small amount of rotational restraint is necessary to prevent web sidesway buckling from occurring.

Table 4: Results for short span joist study with varying deck flexural stiffness and no bottom-chord bridging

	Multiple of Deck Flexural Stiffness Provided By SJI										SJI LRFD Design Load
	0		0.0001		0.001		0.01		1		
	Load	Mode	Load	Mode	Load	Mode	Load	Mode	Load	Mode	
10K1	269	BCY	276	BCY	288	BCY	291	BCY	291	BCY	298
14K3	196	WSB	215	WSB	253	BCY	258	BCY	258	BCY	270
18K3	238	WSB	238	BCY	322	BCY	329	BCY	329	BCY	351

1. Failure loads and SJI LRFD design loads given in lb/ft
2. BCY represents bottom chord yielding failure mode
3. WSB represents web sidesway buckling failure mode

4.2 Bottom-Chord Radius of Gyration on Web Sidesway Buckling

Several members of the SJI have in the past questioned to what degree the out-of-plane radius of gyration of the bottom chord contributes to preventing web sidesway buckling, especially when bottom-chord bridging is provided. Although only three short-span joists were being studied, the authors did attempt to provide some insight to this question by (i) artificially increasing the yield strength of the bottom chord (thereby eliminating bottom-chord yielding as a controlling failure mode), and (ii) systematically varying the bottom-chord radius of gyration. Several analyses were conducted for the joists 10K1, 14K3, and 18K3, but the results were inconclusive. For most of the cases investigated, it was not possible to determine a critical value for the radius of gyration; for the few cases that values were obtained, no consistent pattern was established. It could only be concluded that the radius of gyration does not exclusively control the failure mode of the joist, because it was observed that several interrelated elements (Fig. 17) contribute to the possibility of web sidesway buckling.

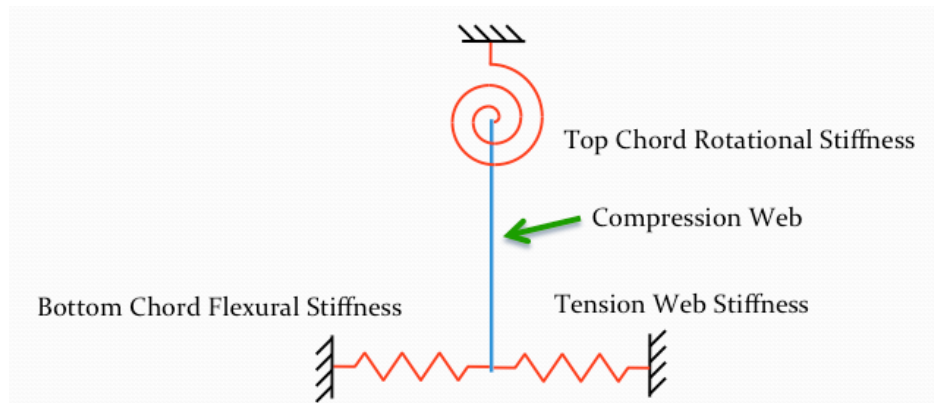


Figure 17: Possible factors contributing to the short span joist failure mode

5. Summary and Conclusions

In this paper, a summary of recent computational research conducted for the Steel Joist Institute on short- and medium-span open-web steel joists is presented. This work includes investigations of horizontal- and x-bridging, gravity and uplift loading, assumed initial imperfections, and web sidesway buckling.

In general, the study indicates that it is feasible to use rigorous second-order elastic finite element analysis to assess the lateral stability behavior of joist systems, including the determination of bridging stiffness and forces used to brace such systems.

More specific conclusions are provided below. It is important to note that these conclusions are based only on the limited number of joist configurations studied.

5.1 Gravity Loading

Studies on systems of parallel joists with horizontal and X-bracing indicated:

- The shape of the initial imperfection used in gravity load analyses should be that of reverse curvature, because it provides a worst-case condition for determining bridging forces and required stiffness. The magnitude of the initial imperfection is directly proportional to the size of the bridging forces.
- An increase in bracing stiffness results in a decrease in bridging forces.

- Due to the lean-on effect, the ideal brace stiffness of a bridging member within a system of joists is significantly greater than the ideal brace stiffness of a single joist.
- Engaging both tension and compression bracing can significantly decrease the required bridging stiffness and forces.
- Computational analysis shows that bridging forces do (to some degree) continue to accumulate over systems of 8 to 10 parallel joists; noting that if all joists in a system lean in the same out-of-plane direction during construction, bridging forces were observed to accumulate linearly.
- The stiffness of the bridging anchorage of the system impacts the required ideal bridging stiffness and forces for the individual joists.
- For X-bracing specifically,
 - providing anchorage reduces both the ideal bracing stiffness and the maximum bracing forces.
 - bridging forces accumulate only slightly due to most of these forces being resolved through a combination of truss action between parallel joists and minor-axis bending of the top- and bottom-chords of these joists.
 - a significantly larger ideal bracing stiffness and maximum bracing force are observed when only tension bracing is assumed engaged.

5.2 Uplift Loading

Investigating similar systems of joists, the following conclusions are made:

- Reverse-curvature imperfections with out-of-plane end panel displacements in the opposite direction of the next bracing location resulted in a worst-case initial imperfection shape for the bottom (compression) chord.
- The additional longitudinal top-chord rotational restraint provided by the flexural stiffness of the deck can result in significant increases (20% to 34%) in the elastic load carrying capacity.
- The additional stiffness provided by the deck can result in a decrease in the required ideal bracing stiffness (85% - 95%).
- The additional stiffness provided by the deck results in a mild decrease (2% - 10%) in bracing force.
- Bracing forces continued to accumulate linearly for the 10-joist systems investigated.
- Engaging both tension and compression bracing results in a significant reduction (50%) in bracing forces when compared to a tension-only system.
- Reducing the applied load results in a fairly linear reduction in bracing forces.
- Likewise, reducing the initial imperfection magnitude results in a linear reduction in bracing forces.
- By including an initial imperfection in only 4 of the 10 parallel joists, the bracing forces are reduced to approximately 40% of the case in which all 10 joists include an imperfection.

5.3 Short Span Joists

With short-span defined by lengths less than 30'-0", the following observations are made for joists subjected to gravity loading:

- When a deck is securely fastened to the top (compression) chord, the number of bridging rows does not significantly affect the load carrying capacity of the joist.
- Web sidesway buckling is almost always the controlling failure mode for joist systems that include a combination of deck attached to the upper chord and no bottom-chord bridging.
- Accounting for only a small fraction of the deck flexural stiffness can significantly increase the load carrying capacity of the joist.
- The degree to which the joist's bottom-chord radius of gyration impacts web sidesway buckling is unclear, because it is only one of several interrelated components that limit the occurrence of this failure.

Acknowledgments

The authors thank the Steel Joist Institute and especially members of the SJI Research Committee for their support and funding of this project. It is important to note that any opinions expressed or conclusions provided in this paper are solely those of the authors and are only based on a relatively small number of joist configurations studied.

References

- Handbook of Steel Construction* (2011). Canadian Institute of Steel Construction, Ontario, Canada.
- MASTAN2 Structural Analysis Program* (2000). www.mastan2.com
- Standard Specifications, Load Tables, and Weight Tables for Steel Joists and Joist Girders* (2005). Steel Joist Institute, Florence, SC.
- Wang, L., Helwig, T. A. (2005). "Critical Imperfections for Beam Bracing Systems." *Journal Of Structural Engineering*, ASCE, 131(6) 933-940.
- Ziemian, R.D., Schwarz, J.E., Emerson, M.E. and Potts, D.R. (2004). "Stability Of Unbraced Steel Joists Subject To Mid-Span Loading." *Proceedings of the American Institute of Steel Construction National Steel Construction Conference and Structural Stability Research Council Technical Session*, Long Beach, CA.